

Multi-objective Optimization in Quantum Parameter Estimation

Beili Gong¹ and Wei Cui^{1,*}

¹*School of Automation Science and Engineering,
South China University of Technology, Guangzhou 510641, China*
(Dated: March 21, 2017)

We study the quantum parameter estimation based on the linear and Kerr-type nonlinear controls in the Hamiltonian of the system. We show that when we enhance the parameter estimation precision, it usually induces significant backaction on the system itself. Moreover, we propose a multi-objective model which aims at optimizing the two conflicting objectives: (1) maximizing the Fisher information that improves the parameter estimation precision; (2) minimizing the backaction on the system that maintains the fidelity. Finally, simulations of a simplified ε -constrained model demonstrate the feasibility of the Hamiltonian control in the quantum parameter estimation.

PACS numbers: 03.65.Yz, 06.20.Dk, 02.30.Yy

I. INTRODUCTION

Quantum information processing and quantum control often require precise information about the parameters in the system Hamiltonian, the surrounding environment, the coupling and measurement strengths, and so on. However, due to inevitable randomness during quantum measurement, and several quantities of interest even cannot correspond to proper quantum observables, the quantum parameter estimation [1–3] has become a fundamental problem in quantum science and technology. Rigorously speaking, this problem arises most especially in gravitational-wave experiments, and the maximum sensitivity for a conventional continuous monitoring of the probe mass's position is given by the standard quantum limit (SQL) for the mass's sensitivity to the classical force [4]. However, Caves [5] showed that with the help of squeezed state technique, quantum mechanical systems can achieve greater sensitivity over the SQL. From then on, scientists and engineers have developed various quantum technologies [6–13] to improve the accuracy of a wide variety of quantum measurements. Theoretically the ultimate precision limit is the Heisenberg limit (HL), which relies on the unitarity of the time evolution. When a quantum state is used as a probe and an optimization procedure is involved, the quantum version of the Cramér-Rao inequality [14–16] can be established. In general, the Cramér-Rao bound can be applied to any parameter estimation problem and the quantum Fisher information (QFI) [17–19] is the upper bound on the precision of parameter estimation.

Be different with the closed quantum system, quantum probes would unavoidably interact with the surrounding environment, which decays the quantum coherence of the probes. In this realistic situation, the dissipative Cramér-Rao bound has been derived, and the estimation accuracy remarkably depends on the underlying dynamical

map with the semigroup property [20]. Due to the profoundness of the theory of open quantum systems [21], enhancing a quantum estimation task in the presence of noise involves the fundamental interest [22–26]. In particular, much attention has been devoted to the estimation of the noisy frequency and loss parameters [27–29]. For example, in recent work [29] it has been shown that the estimation accuracy of loss rate can be improved by the Kerr-type nonlinear Hamiltonian. In this paper, nonlinearity once again reveals its positive role [30] as a resource in the quantum metrology. On the other hand, due to the dissipative evolution of the quantum system, the coherence of the initial state would be quickly damaged and the Gaussian input becomes a set of non-Gaussian states. Thus, how to globally optimize these two conflicting objectives (1. maximizing the Fisher information that improves the parameter estimation precision; 2. minimizing the backaction on the system that maintains the fidelity) is of great importance in practically employing the quantum parameter estimation method.

In our work, we study the quantum parameter estimation based on the linear and Kerr-type nonlinear controls in the Hamiltonian of the system. In particular, the estimation of dissipation rate of a quantum master equation has been considered. With the pure state approximation, we obtain the QFI in analytical form. We verify the validity of this approximation by comparing the approximate QFI with the exact one with various controls (linear and Kerr-type nonlinear). We show that when we enhance the parameter estimation precision, it usually induces significant backaction on the system itself. In this paper, we propose a multi-objective model [31, 32] which can optimize the two conflicting objectives (QFI and fidelity) together. Finally, simulations of a simplified ε -constrained model demonstrate the feasibility of the Hamiltonian control in the quantum parameter estimation.

The paper is organized as follows: in Sec. II, based on a simple quantum master equation, we detailed analysis its solutions with pure state approximation. In Sec. III, we calculate the quantum Fisher information with various control Hamiltonians. In Sec. IV, we study the trade-

*Electronic address: aucuiwei@scut.edu.cn

off between the QFI and the quantum fidelity by the multi-objective optimization theory. We summarize our conclusions in Sec. V.

II. THE MODEL

In reality, the quantum systems are inevitably interacted with the environment, and the evolution of the system is described by a master equation [21]. The simplest master equation describing an amplitude dissipation is

$$\frac{d\rho}{dt} = \gamma \left(a\rho a^\dagger - \frac{1}{2}a^\dagger a\rho - \frac{1}{2}\rho a^\dagger a \right), \quad (1)$$

where γ is the dissipation rate of a bosonic channel, and a is the annihilation operator. Here, we assume that γ is an unknown parameter which required to be estimated. The precision of the parameter estimation is always indicated by the quantum Cramér-Rao inequality [14–16], i.e.,

$$\langle \delta\gamma^2 \rangle \geq \frac{1}{N\mathcal{I}(\gamma)}, \quad (2)$$

where $\mathcal{I}(\gamma)$ is the Fisher information and N is the number of measurements. To improve the parameter estimation precision and also to eliminate the decoherence effect, one can resort to the Hamiltonian control method [16, 19, 33]. Here, we apply the linear control $H_1 = k_1 a^\dagger a$ and Kerr-type nonlinear control [29, 34–36] $H_2 = k_2 (a^\dagger a)^2$ to improve the estimation precision. The Lindblad master equation Eq.(1) can be written as

$$\frac{d\rho}{dt} = -i[H_1 + H_2, \rho] + \gamma \left(a\rho a^\dagger - \frac{1}{2}a^\dagger a\rho - \frac{1}{2}\rho a^\dagger a \right). \quad (3)$$

By denoting the quantities with respect to the loss parameter γ

$$\tau = \gamma t, \quad u_1 = \frac{k_1}{\gamma}, \quad u_2 = \frac{k_2}{\gamma}, \quad (4)$$

the controlled master equation can be described as

$$\begin{aligned} \frac{d\rho}{d\tau} = & -iu_1 [a^\dagger a, \rho] - iu_2 [(a^\dagger a)^2, \rho] \\ & + \left(a\rho a^\dagger - \frac{1}{2}a^\dagger a\rho - \frac{1}{2}\rho a^\dagger a \right). \end{aligned} \quad (5)$$

We assume the initial state of the quantum system is a coherent state, $\rho_0 = |\alpha\rangle\langle\alpha|$. The analytic solution of Eq. (5) in the interaction picture is

$$\rho_I(\tau) = \sum_{l=0}^{\infty} \frac{\left(\frac{1-e^{-\Delta\tau}}{\Delta} \right)^n}{l!} \exp \left\{ -\frac{1}{2}\Delta\tau(p+q) \right\} a_I^\dagger{}^l \rho_{I_0} \left(a_I^\dagger \right)^l$$

where, $a(\tau) = e^{-iu_1\tau a^\dagger a} a_I(\tau) e^{iu_1\tau a^\dagger a}$, and $\Delta = 1 + 2iu_2(p-q)$. Thus, the matrix elements $\rho_{p,q}$ of Eq. (5)

can be denoted as,

$$\begin{aligned} \rho_{p,q} = & \lambda \exp \left\{ -\frac{1}{2}\Delta\tau(p+q) \right\} \\ & \times \exp \left\{ -iu_1\tau(p-q) - |\alpha|^2 \left(1 - \frac{1-e^{-\Delta\tau}}{\Delta} \right) \right\}, \\ & \text{for } p, q = 0, 1, 2, 3, \dots \end{aligned} \quad (6)$$

where $\lambda = \alpha^p \bar{\alpha}^q / \sqrt{p!q!}$, and $\bar{n} = |\alpha|^2$. Below, we consider several specific cases.

(i) When $u_1 = u_2 = 0$, i.e., $k_1 = k_2 = 0$, the quantum system will free evolved without control, and the elements of the density matrix are

$$\rho_{p,q} = \lambda \exp \left\{ -\frac{1}{2}\tau(p+q) - |\alpha|^2 e^{-\tau} \right\}. \quad (7)$$

The lowest order of expansion can be approximately rewritten as a pure state $\tilde{\rho} = |\psi_\gamma\rangle\langle\psi_\gamma|$, where

$$|\psi_\gamma\rangle_{\text{free}} = \exp \left\{ -\frac{1}{2}|\alpha|^2 e^{-\tau} \right\} \left[\alpha \exp \left\{ -\frac{1}{2}\tau \right\} \right]. \quad (8)$$

(ii) When $u_1 \neq 0$, $u_2 = 0$, i.e., $k_1 \neq 0$, $k_2 = 0$, the system will controlled by the linear control H_1 , and the elements of the density matrix are

$$\rho_{p,q} = \lambda \exp \left\{ -\frac{1}{2}\tau(p+q) - |\alpha|^2 e^{-\tau} - iu_1\tau(p-q) \right\}. \quad (9)$$

The lowest order of expansion can be approximately rewritten by a pure state $\tilde{\rho} = |\psi_\gamma\rangle\langle\psi_\gamma|$, where

$$|\psi_\gamma\rangle_{\text{linear}} = \exp \left\{ -\frac{1}{2}|\alpha|^2 e^{-\tau} \right\} \left[\alpha \exp \left\{ -\frac{1}{2}\tau - iu_1\tau \right\} \right]. \quad (10)$$

(iii) When $u_1 = 0$, $u_2 \neq 0$, i.e., $k_1 = 0$, $k_2 \neq 0$, the system will only controlled by the Kerr-type nonlinear control H_2 , the elements of the density matrix are

$$\rho_{p,q} = \lambda \exp \left\{ -\frac{1}{2}\Delta\tau(p+q) - |\alpha|^2 \left(1 - \frac{1-e^{-\Delta\tau}}{\Delta} \right) \right\}. \quad (11)$$

The lowest order of expansion can be approximately rewritten as a pure state $\tilde{\rho} = |\psi_\gamma\rangle\langle\psi_\gamma|$, where

$$\begin{aligned} |\psi_\gamma\rangle_{\text{Kerr}} = & \exp \left\{ -\frac{1}{2}|\alpha|^2 e^{-\tau} \right\} \times \\ & \left[\alpha \exp \left\{ -\frac{1}{2}\tau - iu_2\tau - iu_2|\alpha|^2\tau^2 \right\} \right]. \end{aligned} \quad (12)$$

(iv) Finally, it is clear that when $u_1 \ll 1$ and $u_2 \ll 1$, the quantum state can be approximated to

$$\begin{aligned} \rho_{p,q} = & \lambda \exp \left\{ -\frac{1}{2}\tau(p+q) - |\alpha|^2 e^{-\tau} \right\} \exp \left\{ -iu_1\tau(p-q) \right. \\ & \left. - iu_2\tau(p^2 - q^2) - iu_2|\alpha|^2\tau^2(p-q) \right\}, \end{aligned} \quad (13)$$

by expansion of the exponent in Eq. (6) for small τ . The lowest order of expansion can be approximately rewritten as a pure state $\tilde{\rho} = |\psi_\gamma\rangle\langle\psi_\gamma|$, where

$$|\psi_\gamma\rangle_{\text{cont}} = \exp\left\{-\frac{1}{2}|\alpha|^2 e^{-\tau}\right\} \times \left[\frac{1}{\alpha \exp\left\{-\frac{1}{2}\tau - i(u_1 + u_2)\tau - iu_2\tau^2|\alpha|^2\right\}} \right]. \quad (14)$$

III. QUANTUM PARAMETER ESTIMATION

According to the quantum Cramér-Rao inequality Eq. (2), the quantum Fisher information

$$\mathcal{I}(\gamma) = \text{Tr}[\rho L_\gamma^2] \quad (15)$$

provides a satisfactory way to calculate the estimation precision. Here, L_γ is called the *system logarithmic derivative* [37], which satisfies

$$\partial_\gamma \rho = \frac{L_\gamma \rho_\gamma + \rho_\gamma L_\gamma}{2}.$$

Diagonalization of the density operator ρ can simplify the quantum Fisher information (QFI), i.e, if $\rho = \sum_n p_n |\psi_n\rangle\langle\psi_n|$ for some $p_n, |\psi_n\rangle$, where $\sum_n p_n = 1$, the QFI can be written as

$$\mathcal{I}(\gamma) = 2 \sum_{n,m} \frac{|\langle\psi_m|\partial_\gamma \rho_\gamma|\psi_n\rangle|^2}{p_m + p_n}, \quad (16)$$

where $p_m + p_n \neq 0$ for all n, m . Moreover, for a pure state $\tilde{\rho}_\gamma^2 = \tilde{\rho}_\gamma$, Eq. (16) can be rewritten as

$$\mathcal{I}(\gamma) = 4 \left[\langle\partial_\gamma \psi_\gamma|\partial_\gamma \psi_\gamma\rangle - (\langle\psi_\gamma|\partial_\gamma \psi_\gamma\rangle)^2 \right]. \quad (17)$$

Partial derivation with respect to γ over the four pure states Eqs. (8), (10), (12), and (14) gives,

$$|\partial_\gamma \psi_\gamma\rangle_{\text{free}} = t \exp\left\{-\frac{1}{2}|\alpha|^2 e^{-\tau}\right\} \times \left[\frac{\frac{1}{2}|\alpha|^2 e^{-\tau}}{\alpha \left(\frac{1}{2}|\alpha|^2 e^{-\tau} - \frac{1}{2}\right) \exp\left\{-\frac{1}{2}\tau\right\}} \right]; \quad (18)$$

$$|\partial_\gamma \psi_\gamma\rangle_{\text{linear}} = t \exp\left\{-\frac{1}{2}|\alpha|^2 e^{-\tau}\right\} \times \left[\frac{\frac{1}{2}|\alpha|^2 e^{-\tau}}{\alpha \left(\frac{1}{2}|\alpha|^2 e^{-\tau} - \frac{1}{2} - iu_1\right) \exp\left\{-\frac{1}{2}\tau - iu_1\tau\right\}} \right]; \quad (19)$$

$$|\partial_\gamma \psi_\gamma\rangle_{\text{Kerr}} = t \exp\left\{-\frac{1}{2}|\alpha|^2 e^{-\tau}\right\} \times \left[\frac{\frac{1}{2}|\alpha|^2 e^{-\tau}}{\alpha \left(\frac{1}{2}|\alpha|^2 e^{-\tau} - \frac{1}{2} - iu_2 - 2iu_2|\alpha|^2\tau\right) \exp(M)} \right], \quad (20)$$

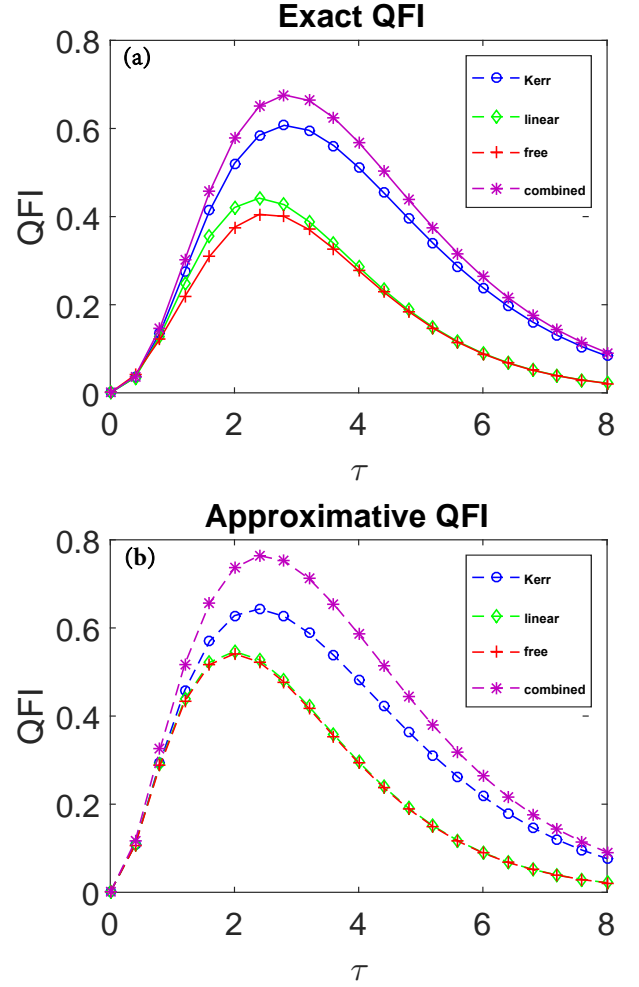


FIG. 1: (Color online) The evolution of quantum Fisher information for the dissipation rate estimation with various control Hamiltonians. Here, the red-cross curves demonstrate the free evolution without control; the green-diamond curves show the evolution with linear control H_1 ; the blue-circle curves exhibit the evolution with Kerr-type nonlinear control; the purple-star curves represent the evolution with both linear and Kerr-type nonlinear controls. In Fig. (a), we directly plot the QFIs as a function of the rescaled time τ based on the first ten orders of the elements of the density matrix Eq. (6). We regard these as exact QFIs. In Fig. (b), we plot the evolution of the QFIs, Eqs. (22)-(25), with the pure state approximation. Here, we choose the mean energy $\bar{n} = 1$, and $u_1 = u_2 = 0.05$.

here $M = -\frac{1}{2}\tau - iu_2\tau - iu_2|\alpha|^2\tau^2$; and

$$|\partial_\gamma \psi_\gamma\rangle_{\text{cont}} = t \exp\left\{-\frac{1}{2}|\alpha|^2 e^{-\tau}\right\} \times \left[\frac{\frac{1}{2}|\alpha|^2 e^{-\tau}}{\alpha \left(\frac{1}{2}|\alpha|^2 e^{-\tau} - \frac{1}{2} - i(u_1 + u_2) - 2iu_2|\alpha|^2\tau\right) \exp(N)} \right], \quad (21)$$

here $N = -\frac{1}{2}\tau - i(u_1 + u_2)\tau - iu_2|\alpha|^2\tau^2$, respectively. Thus, according to Eq. (17) we calculate the QFIs for

the four cases.

$$\begin{aligned}
\mathcal{I}_{\text{free}}(\tau) &= \frac{\tau^2}{\gamma^2} \exp\left\{-|\alpha|^2 e^{-\tau}\right\} \left[|\alpha|^4 e^{-2\tau} + |\alpha|^2 e^{-\tau} \left(|\alpha|^2 e^{-\tau} - 1\right)^2 \right] \\
&\quad - \frac{\tau^2}{\gamma^2} \exp\left\{-2|\alpha|^2 e^{-\tau}\right\} |\alpha|^4 e^{-2\tau} \left(|\alpha|^2 e^{-\tau}\right)^2 \\
&\approx \frac{\tau^2}{\gamma^2} |\alpha|^2 e^{-\tau},
\end{aligned} \tag{22}$$

$$\begin{aligned}
\mathcal{I}_{\text{linear}}(\tau) &= 4 \frac{\tau^2}{\gamma^2} \exp\left\{-|\alpha|^2 e^{-\tau}\right\} \left[\frac{1}{4} |\alpha|^4 e^{-2\tau} + |\alpha|^2 e^{-\tau} \left(\frac{1}{4} \left(|\alpha|^2 e^{-\tau} - 1\right)^2 + u_1^2 \right) \right] \\
&\quad - 4 \frac{\tau^2}{\gamma^2} \exp\left\{-2|\alpha|^2 e^{-\tau}\right\} |\alpha|^4 e^{-2\tau} \left(\frac{1}{4} |\alpha|^4 e^{-2\tau} + u_1^2 \right) \\
&\approx \frac{\tau^2}{\gamma^2} |\alpha|^2 e^{-\tau} \left(1 + 4u_1^2 \right),
\end{aligned} \tag{23}$$

$$\begin{aligned}
\mathcal{I}_{\text{Kerr}}(\tau) &= 4 \frac{\tau^2}{\gamma^2} \exp\left\{-|\alpha|^2 e^{-\tau}\right\} \left[\frac{1}{4} |\alpha|^4 e^{-2\tau} + |\alpha|^2 e^{-\tau} \left(\frac{1}{4} \left(|\alpha|^2 e^{-\tau} - 1\right)^2 + u_2^2 \left(2|\alpha|^2 \tau + 1 \right)^2 \right) \right] \\
&\quad - 4 \frac{\tau^2}{\gamma^2} \exp\left\{-2|\alpha|^2 e^{-\tau}\right\} |\alpha|^4 e^{-2\tau} \left(\frac{1}{4} |\alpha|^4 e^{-2\tau} + u_2^2 \left(1 + 2|\alpha|^2 \tau \right)^2 \right) \\
&\approx \frac{\tau^2}{\gamma^2} |\alpha|^2 e^{-\tau} \left(1 + 16u_2^2 |\alpha|^4 \tau^2 \right),
\end{aligned} \tag{24}$$

$$\begin{aligned}
\mathcal{I}_{\text{cont}}(\tau) &= 4 \frac{\tau^2}{\gamma^2} \exp\left\{-|\alpha|^2 e^{-\tau}\right\} \left[\frac{1}{4} |\alpha|^4 e^{-2\tau} + |\alpha|^2 e^{-\tau} \left(\frac{1}{4} \left(|\alpha|^2 e^{-\tau} - 1\right)^2 + (u_1 + u_2 + 2\tau |\alpha|^2 u_2)^2 \right) \right] \\
&\quad - 4 \frac{\tau^2}{\gamma^2} \exp\left\{-2|\alpha|^2 e^{-\tau}\right\} |\alpha|^4 e^{-2\tau} \left[\frac{1}{4} |\alpha|^4 e^{-2\tau} + \left(u_1 + u_2 + 2u_2 \tau |\alpha|^2 \right)^2 \right] \\
&\approx \frac{\tau^2}{\gamma^2} |\alpha|^2 e^{-\tau} \left(1 + 4 \left(u_1 + u_2 + 2\tau |\alpha|^2 u_2 \right)^2 \right).
\end{aligned} \tag{25}$$

Here the simplified QFIs are obtained by omitting the higher-order terms. We regard these QFIs as pure state approximations. To testify the validity of the pure state approximation, we also directly calculate the QFIs based on the first ten orders of the elements of the density matrix Eq. (6). We regard these as exact QFIs. In Fig. 1, we plot the evolution of the QFI with various control Hamiltonians. Here, we choose the mean energy $\bar{n} = 1$, and $u_1 = u_2 = 0.05$. The red-cross curves demonstrate the free evolution without control; the green-diamond curves show the evolution with linear control H_1 ; the blue-circle curves exhibit the evolution with Kerr-type nonlinear control; the purple-star curves represent the evolution with both linear and Kerr-type nonlinear controls. In Fig. 1(a), we directly plot the QFIs as a function of the rescaled time τ based on the first ten orders of the

elements of the density matrix Eq. (6). In Fig. 1(b), we plot the evolution of the QFIs, Eqs. (22)–(25), with the pure state approximation. The comparison between the two figures shows the effectiveness of the pure state approximation. Thus, we will optimize the control input based on the pure state approximated QFIs, Eqs. (22)–(25).

Below we calculate the information lose during the parameter estimation process by the quantum fidelity, a measure of the closeness of two quantum states, $F(\rho_0, \rho) = (\text{Tr}(\sqrt{\sqrt{\rho_0}\rho\sqrt{\rho_0}}))^2$. It is clear that the fidelity is symmetric with respect to ρ_0 and ρ , and ranges from 0 to 1, i.e., $F \in [0, 1]$. Furthermore, $F = 0$ if and only if ρ_0 and ρ are orthogonal and $F = 1$ if and only if $\rho_0 = \rho$. If $\rho_0 = |\varphi\rangle\langle\varphi|$, $\rho = |\psi\rangle\langle\psi|$ are pure states, the fidelity is reduced to a relative simple form $F = |\langle\psi|\varphi\rangle|^2$.

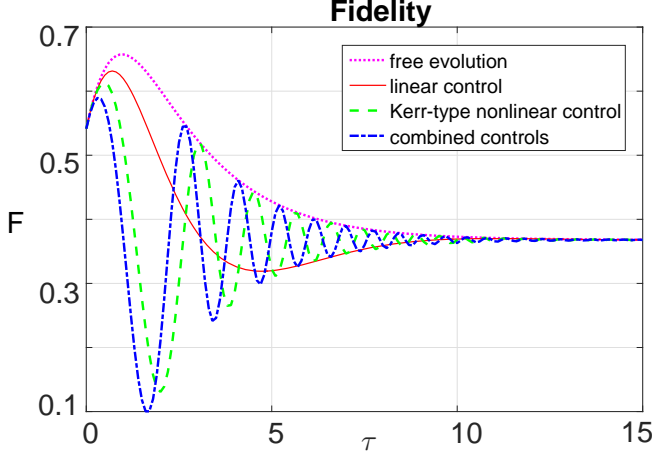


FIG. 2: (Color line) The time evolution of the fidelity with various control Hamiltonians. The purple dotted curve is the free evolution without control. The red solid curve represents the evolution with linear control. The green dashed curve indicate the evolution with Kerr-type nonlinear control. The blue dash-dotted curve represents the evolution with both linear and Kerr-type nonlinear control.

Thus, during the estimation process, based on Eq. (14) we have the quantum state fidelity at time τ

$$F(\tau) = \left| \exp \left\{ -\frac{1}{2}|\alpha|^2 - \frac{1}{2}|\alpha|^2 e^{-\tau} \right\} \left[1 + |\alpha|^2 \exp \left\{ -\frac{1}{2}\tau + i(u_1 + u_2)\tau + iu_2\tau^2|\alpha|^2 \right\} \right] \right|^2. \quad (26)$$

In Fig. 2, we plot the evolution of the fidelity as a function of the rescaled time τ with various control Hamiltonians. The purple dotted curve is the free evolution without control. The red solid curve represents the evolution with linear control. The green dashed curve indicate the evolution with Kerr-type nonlinear control. The blue dash-dotted curve represents the evolution with both linear and Kerr-type nonlinear control. Here, the parameters are $|\alpha|^2 = 1$, $u_1 = 0.5$, $u_2 = 0.5$. The figure shows that when we enhance the parameter estimation precision, it of course induces significant backaction on the system itself. Obviously then the multi-objective optimization is to measure on a time scale where both the parameter estimation precision is relatively high and the backaction is low.

IV. MULTI-OBJECTIVE OPTIMIZATION

The results in Sec. III show a clear trade-off relation between the parameter estimation precision and the fidelity. Here, we have two conflicting objectives that need to be optimized. In [38], the second author of this article and co-authors used the Goal Programming to deal with

the similar problem in quantum state reconstruction. Instead of finding solutions which absolutely minimize or maximize objective functions, the task of goal programming is to find solutions that, if possible, satisfy a set of goals, or otherwise violate the goals minimally. In this article, we use the multi-objective optimization [31, 32] method to deal with this problem. A multi-objective optimization problem can be formulated as

$$\begin{aligned} &\text{Minimize} && (f_1(x), f_2(x), \dots, f_k(x)) \\ &\text{subject to} && x \in X, \end{aligned} \quad (27)$$

where we have $k (\geq 2)$ objective functions $\{f_1, f_2, \dots, f_k\}$. The decision vector $x = [x_1, x_2, \dots, x_n]^T$ belongs to the feasible set X . Because of the contradiction of the objectives $f_1(x), f_2(x), \dots, f_k(x)$, it is not possible to find a single solution that would be optimal for all the objectives simultaneously. The common solution is the so-called Pareto front which means there does not exist another solution that dominates it [31, 32]. There are usually a lot of Pareto optimal solutions. The solution set can be nonconvex and nonconnected. Formulating a single-objective optimization problem is a feasible efficient way such that optimal solutions to the single-objective optimization problem are Pareto optimal solutions to the original multi-objective optimization problem. ε -constraint is one of the scalarizing methods:

$$\begin{aligned} &\text{Minimize} && f_j(x) \\ &\text{subject to} && \begin{cases} x \in X \\ f_i(x) \leq \varepsilon_j \text{ for } i \in \{1, \dots, k\} \setminus \{j\}. \end{cases} \end{aligned} \quad (28)$$

In our optimization task, the decision vector is defined as $x = [\tau, u_1, u_2, |\alpha|^2]^T$. In order to simplify the discussion, let's take partial derivative of quantum Fisher informations, i.e., Eqs. (22-25), with respect to τ and let the results be 0. This is reasonable because the maximum value of the Fisher information is of particular interest in the quantum parameter estimation precision. Thus, we obtain the maximum values $\mathcal{I}_{\text{free}}^*$, $\mathcal{I}_{\text{linear}}^*$, $\mathcal{I}_{\text{Kerr}}^*$, and $\mathcal{I}_{\text{cont}}^*$:

$$\mathcal{I}_{\text{free}}^* \approx \frac{4|\alpha|^2}{\gamma^2} e^{-2}, \quad (29)$$

$$\mathcal{I}_{\text{linear}}^* \approx \frac{4|\alpha|^2}{\gamma^2} e^{-2} \left(1 + 4u_1^2 \right), \quad (30)$$

$$\mathcal{I}_{\text{Kerr}}^* \approx \frac{4|\alpha|^2}{\gamma^2} e^{-2} \left(1 + 64u_2^2 |\alpha|^2 \right), \quad (31)$$

$$\mathcal{I}_{\text{cont}}^* \approx \frac{4|\alpha|^2}{\gamma^2} e^{-2} \left(1 + 4 \left(u_1 + u_2 + 4|\alpha|^2 u_2 \right)^2 \right). \quad (32)$$

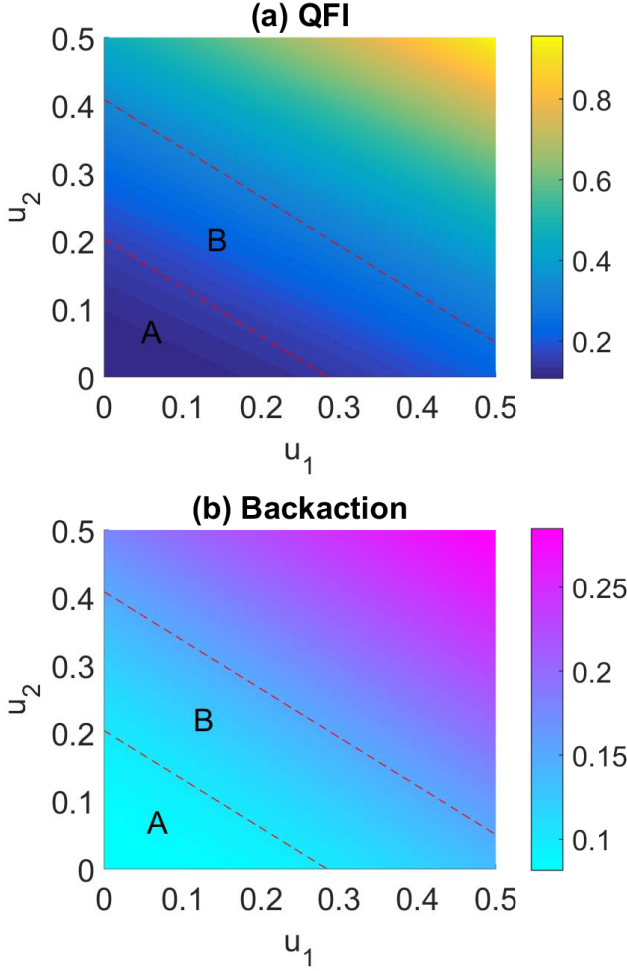


FIG. 3: (Color online) Illustration of the ε -constrained multi-objective optimization for quantum parameter estimation. In (a) and (b), the Fisher information $\mathcal{I}_{\text{cont}}^*$ and the backaction \mathcal{B} as functions of the linear and Kerr-type nonlinear controls are plotted, when $|\alpha|^2 = 0.2$. In Fig. 3(b), region A and region B indicate the constraints $\varepsilon = 0.10$ and $\varepsilon = 0.15$, respectively. Thus, the ε -constrained optimum value of the quantum Fisher information is restricted in A or B in Fig. 3(a).

Here the extreme points τ^* are 2, which is the solution of following equations:

$$-16u_2^2|\alpha|^4\tau^{*3} + 64u_2^2|\alpha|^4\tau^{*2} - \tau^* + 2 = 0, \quad (33)$$

$$-4T^2\tau^* + 8T^2 + 16|\alpha|^2u_2T\tau^* - \tau^* + 2 = 0, \quad (34)$$

$$\text{with } T = u_1 + u_2 + 2|\alpha|^2u_2\tau^*.$$

Because of $u_1 \ll 1$, $u_2 \ll 1$, approximate solutions of Eq. (33) and Eq. (34) are 2. In Fig. 1 we can also find that the maximum values are achieved around $\tau = 2$. It is clear that the quantum Fisher information is a monotonically increasing function of the linear and Kerr-type nonlinear controls, u_1 , u_2 , and $|\alpha|^2$. On the other hand,

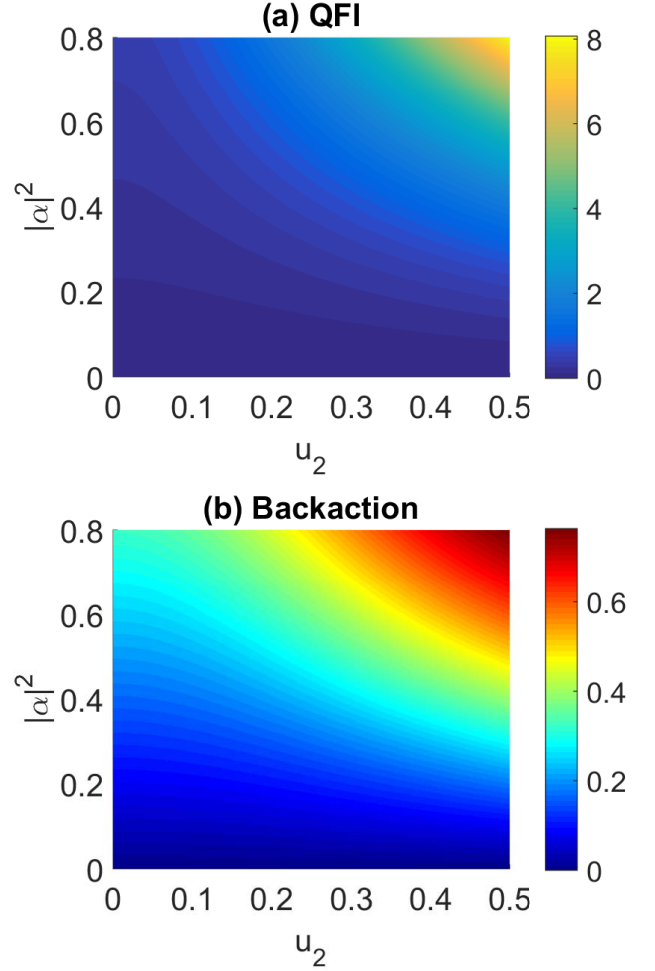


FIG. 4: (Color online) In Fig. 4(a) and Fig. 4(b) the Fisher information $\mathcal{I}_{\text{cont}}^*$ and the backaction \mathcal{B} as functions of the Kerr-type nonlinear control and the parameter $|\alpha|^2$ are plotted, respectively.

at the same time the backaction to the quantum state is

$$\begin{aligned} \mathcal{B} &= 1 - F|_{\tau=\tau^*} \\ &\approx 1 - \left| \exp \left\{ -\frac{1}{2}|\alpha|^2 - \frac{1}{2}|\alpha|^2 e^{-2} \right\} \right. \\ &\quad \left. \left[1 + |\alpha|^2 \exp \left\{ -1 + 2i(u_1 + u_2) + 4iu_2|\alpha|^2 \right\} \right] \right|^2. \end{aligned} \quad (35)$$

Finally, we arrive at the ε -constrained multi-objective optimization problem,

$$\begin{aligned} &\text{Maximum } \mathcal{I}^* \\ &\text{subject to } \begin{cases} \mathcal{B} \leq \varepsilon \\ u_1, u_2, |\alpha|^2 \in [0, 1]. \end{cases} \end{aligned} \quad (36)$$

The parameter ε is regarded as the permissible damage of the initial state.

In Fig. 3, we plot the quantum Fisher information $\mathcal{I}_{\text{cont}}^*$ and the backaction $\mathcal{B} = 1 - F$ as functions of the linear

control u_1 and Kerr-type nonlinear control u_2 . Here the parameter $|\alpha|^2 = 0.2$. Choose permissible damage ε , a control region $u_1 \times u_2$ is generated in Fig. 3(b). Then in this region, one can optimize the quantum Fisher information in Fig. 3(a). As an example, in Fig. 3(b) region A and region B indicate the constraints $\varepsilon = 0.10$ and $\varepsilon = 0.15$, respectively. Thus, the ε -constrained optimum value of the quantum Fisher information is restricted in A or B in Fig. 3(a). As we show above, the Fisher information is a monotonically increasing function of the linear and Kerr-type nonlinear controls. Thus, the ε -constrained optimum values of the quantum Fisher information are located in the front dashed lines. In Fig. 4, only the Kerr-type nonlinear control is employed. The parameter $|\alpha|^2$ also plays an important role in optimizing the Fisher information in quantum parameter estimation. These simulation results demonstrate the feasibility of Hamiltonian control in enhancing the quantum parameter estimation precision.

V. CONCLUSION

In many realistic quantum systems, the reliability of the quantum parameter estimation is an important is-

sue. In this article we employed the linear and Kerr-type nonlinear controllers to improve the estimation precision of unknown parameters that govern the system evolution. In particular, the estimation of the dissipation rate of a quantum master equation has been considered. We show that when we enhance the parameter estimation precision, it usually induces significant backaction on the system itself. We propose a multi-objective model to maximize the Fisher information, and also to minimize the backaction on the quantum system. Finally, simulations of a simplified ε -constrained model demonstrate the feasibility of the Hamiltonian control in the quantum parameter estimation.

ACKNOWLEDGEMENTS

This work is supported by the National Natural Science Foundation of China under Grant 11404113, and the Guangzhou Key Laboratory of Brain Computer Interaction and Applications under Grant 201509010006.

-
- [1] C. W. Helstrom, *Quantum Detection and Estimation Theory*, (Academic Press, New York, 1976).
 - [2] H. M. Wiseman and G. J. Milburn, *Quantum Measurements and Control*, (Cambridge University, Cambridge, 2010).
 - [3] A. Holevo, *Probabilistic and Statistical Aspects of Quantum Theory*, (Edizioni della Normale, 2011).
 - [4] V. B. Braginsky and F. Ya. Khalili, *Quantum Measurement*, (Cambridge University Press, Cambridge, 1992).
 - [5] C. M. Caves, Phys. Rev. D **23**, 1693 (1981).
 - [6] V. Giovannetti, S. Lloyd, and L. Maccone, Science **306**, 1330 (2004).
 - [7] V. Giovannetti, S. Lloyd, and L. Maccone, Phys. Rev. Lett. **96**, 010401 (2006).
 - [8] N. B. Lovett, C. Crosnier, M. Perarnau-Llobet, and B. C. Sanders, Phys. Rev. Lett. **110**, 220501 (2013).
 - [9] G. R. Jin, W. Yang, and C. P. Sun, Phys. Rev. A **95**, 013835 (2017).
 - [10] J. Cheng, Phys. Rev. A **90**, 063838 (2014).
 - [11] L. Zhang, A. Datta, and Ian A. Walmsley, Phys. Rev. Lett. **114**, 210801 (2015).
 - [12] M. Zwiars, C. A. Pérez-Delgado, and P. Kok, Phys. Rev. Lett. **105**, 180402 (2010).
 - [13] L. Pezzé and A. Smerzi, Phys. Rev. Lett. **99**, 223602 (2007).
 - [14] S. L. Braunstein and C. M. Caves, Phys. Rev. Lett. **72**, 3439 (1994).
 - [15] M. G. A. Paris, Int. J. Quant. Inf. **7**, 125 (2009).
 - [16] K. Jacobs, *Quantum Measurement Theory and its Applications*, (Cambridge University, Cambridge, 2014).
 - [17] X. M. Lu, X. G. Wang, and C. P. Sun, Phys. Rev. A **82**, 042103 (2010).
 - [18] Z. H. Wang, Q. Zheng, X. G. Wang, and Y. Li, Sci. Rep. **6**, 22347 (2016).
 - [19] H. Yuan, C.-H. F. Fung, Phys. Rev. Lett. **115**, 110401 (2015).
 - [20] S. Alipour, M. Mehboudi, and A. Reza khani, Phys. Rev. Lett. **112**, 120405 (2014).
 - [21] H. P. Breuer and F. Petruccione, *The Theory of Open Quantum Systems*, (Oxford University, New York, 2002).
 - [22] B. M. Escher, R. L. de M. Filho, and L. Davidovich, Nature Phys. **7**, 406 (2011).
 - [23] M. Tsang, New J. Phys. **15**, 073005 (2013).
 - [24] R. Nair, M. Tsang, Phys. Rev. Lett. **117**, 190801 (2016).
 - [25] S. Gammelmark and K. Mølmer, Phys. Rev. A **87**, 032115 (2013).
 - [26] A. H. Kiilerich and K. Mølmer, Phys. Rev. A **94**, 032103 (2016).
 - [27] A. Smirne, J. Kołodziej, S. F. Huelga, and R. Demkowicz-Dobrzański, Phys. Rev. Lett. **116**, 120801 (2016).
 - [28] G. Spedalieri, S. L. Braunstein, and S. Pirandola, "Thermal quantum metrology", arXiv:1602.05958 (2016).
 - [29] M. A. C. Rossi, F. Albarelli, and M. G. A. Paris, Phys. Rev. A **93**, 053805 (2016).
 - [30] M. G. Genoni, C. Invernizzi, and M. G. Paris, Phys. Rev. A **80**, 033842 (2009).
 - [31] M. Ehrgott, *Multicriteria Optimization*, (Springer, Berlin, 2005).
 - [32] K. M. Miettinen, *Nonlinear Multiobjective Optimization*, (Kluwer Academic Publishers, Norwell, 1999).
 - [33] D. J. Egger and F. K. Wilhelm, Phys. Rev. Lett. **112**, 240503 (2014).

- [34] R. Boyd, *Nonlinear Optics*, 3rd ed. (Academic Press, Burlington, MA, 2008).
- [35] M. Stobińska, G. J. Milburn, and K. Wódkiewicz, Phys. Rev. A **78**, 013810 (2008).
- [36] G. J. Milburn and C. A. Holmes, Phys. Rev. Lett. **56**, 2237 (1986).
- [37] M. A. Ciampini, N. Spagnolo, C. Vitelli, L. Pezzè, A. Smerzi, and F. Sciarrino, Sci. Rep. **6**, 28881 (2016).
- [38] W. Cui, N. Lambert, Y. Ota, X. Y. Lu, Z. L. Xiang, J. Q. You, and F. Nori, Phys. Rev. A **86**, 052320 (2012).